Journal of Cystic Fibrosis 16 (2017) 275–282

www.elsevier.com/locate/jcf

Original Article

Hyperpolarized ^{129}Xe for investigation of mild cystic fibrosis lung disease in pediatric patients

Robert P. Thomen [a,b], Laura L. Walkup [a], David J. Roach [a], Zackary I. Cleveland [a,c], John P. Clancy [c], Jason C. Woods [a,b,c,*]

[a] Center for Pulmonary Imaging Research, Cincinnati Children's Hospital Medical Center, Cincinnati, OH, United States
[b] Department of Physics, Washington University in St. Louis, St. Louis, MO, United States
[c] Division of Pulmonary Medicine, Cincinnati Children's Hospital, Cincinnati, OH, United States

Received 26 March 2016; revised 15 July 2016; accepted 17 July 2016
Available online 29 July 2016

Abstract

Background: Cystic fibrosis (CF) is a genetic disease which carries high morbidity and mortality from lung-function decline. Monitoring disease progression and treatment response in young patients is desirable, but serial imaging via CT is often considered prohibitive, and detailed functional information cannot be obtained using conventional imaging techniques. Hyperpolarized ^{129}Xe magnetic resonance imaging (MRI) can depict and quantify regional ventilation, but has not been investigated in pediatrics. We hypothesized that ^{129}Xe MRI is feasible and would demonstrate ventilation defects in mild CF lung disease with greater sensitivity than FEV_1.

Methods: 11 healthy controls (age 6–16 years) and 11 patients with mild CF (age 8–16 years, Forced Expiratory Volume (FEV_1) percent predicted >70%) were recruited for this study. Nine CF patients had an FEV_1 > 85%. Each subject was imaged via hyperpolarized ^{129}Xe MRI, and the ventilation defect percentage (VDP) was measured. FEV_1 and VDP were compared between the groups.

Results: FEV_1 for controls was 100.3% ± 8.5% (mean ± sd) and for CF patients was 97.9% ± 16.0% ($p = 0.67$). VDP was 6.4% ± 2.8% for controls and 18.3% ± 8.6% for CF ($p < 0.001$). When considering the 9 CF patients with normal FEV_1 (>85%), the mean FEV_1 was 103.1% ± 12.3% ($p = 0.57$ compared to controls) and VDP was 15.4% ± 6.3% ($p = 0.002$).

Conclusions: Hyperpolarized ^{129}Xe MRI demonstrated ventilation defects in CF patients with normal FEV_1 and more effectively discriminated CF from controls than FEV_1. Thus ^{129}Xe may be a useful outcome measure to detect mild CF lung disease, to investigate regional lung function in pediatric lung diseases, and to follow disease progression.

Keywords: Hyperpolarized; Mri; Cystic fibrosis; Pediatric

1. Introduction

Cystic Fibrosis (CF) is a genetic disorder caused by mutations on the cystic fibrosis transmembrane conductance regulator (CFTR) which disrupts airway epithelial ion transport and mucus production, resulting in thick mucus accumulation, infection, inflammation, and airway obstruction. CF affects over 70,000 people worldwide, carries a median survival slightly over 40 years, and requires lifelong management with pulmonary and nutrition-focused therapies [1,2]. While several organs are impacted by CF, pulmonary morbidities are responsible for at least 80% of all CF-related deaths [3]. Because mucus retention, infection, and inflammation are largely responsible for decline in lung function, disease management typically includes therapies targeting these processes. CF airway obstruction is a regional process, supporting the use of imaging techniques (mostly CT) for diagnosis, investigation, and monitoring of regional structural pathology. What is lacking from current techniques is the ability to detect and monitor detailed functional information in the lungs — a gap which hyperpolarized-gas MRI is well-suited to fill.

* Corresponding author at: CPIR, Cincinnati Children's Hospital Medical Center, ML-5033, Cincinnati, OH 45229, United States.
E-mail address: Jason.woods@cchmc.org (J.C. Woods).

http://dx.doi.org/10.1016/j.jcf.2016.07.008

As proven pulmonary treatments are being examined and extended into patients at early ages for disease prevention, it is vital to diagnose, understand, and monitor pathologies in early CF lung disease to more effectively tailor individualized treatments and study efficacy of emerging therapies. Treatment goals have shifted towards early prevention and limitation of more severe and irreversible abnormalities (e.g., bronchiectasis) but tools are lacking to detect and monitor regional lung function. There is a pressing need for sensitive measures of regional lung disease that can be employed for personalizing treatment regimens, for use in early phase clinical trials that serve as a robust biomarker of intervention efficacy, and for the conduct of studies with small cohorts of patients with rare CF-causing mutations (such as patients with gating mutations and other mutations responsive to the potentiator ivacaftor - approximately 6% of the total CF population) [4].

CT (computed tomography) is currently the gold standard in research for investigation of regional structural pathology in CF [5], but because it involves exposure to ionizing radiation, its use is limited in pediatrics and in longitudinal research studies. Recent advances in ultra-short echo (UTE) MRI sequences have brought MRI into strong competition with CT for obtaining high-resolution structural images, but even the highest-quality CT or MR images provide only structural information [6]. The multiple inert gas elimination technique (MIGET) involves precise measurement of partial pressures of various inert gases during inhalation and after exhalation to quantify ventilation and ventilation/perfusion ratios [7]. One of these measures via multiple breath washout, lung clearance index (LCI), has been shown to have greater sensitivity than FEV_1 to detect ventilation inhomogeneity in mild CF lung disease, but is a global measure which cannot provide spatial information [8,9].

In the past 20 years, hyperpolarized (HP) gas MRI (using either ^{3}He or ^{129}Xe) of lung has been shown to be a sensitive imaging tool for investigation of lung function [10–12]. Several groups have performed HP ^{3}He MRI in CF patients (mostly adults) in order to investigate regional defects in ventilation [13–16], HP gas repeatability [17,18], longitudinal ventilation changes [19], and treatment efficacy [20–23]. Use of ^{129}Xe in pediatrics is more restricted than ^{3}He due to its slightly higher Ostwald solubility (ratio of gas volume absorbed by a liquid to the liquid volume) and thus greater anesthetic effect at high doses, but recent studies have shown that single-breath-holds of sub-anesthetic doses of Xe present no safety concerns in adults [24] or children [25]. Because of the increasing cost and scarcity of ^{3}He, HP gas research has recently shifted focus towards ^{129}Xe [26,27], and indeed, there is some evidence that ^{129}Xe may be more sensitive than ^{3}He to early functional deficits, [26] but CF research in pediatrics with HP ^{129}Xe MRI has not been reported.

In this work we hypothesized that ^{129}Xe MRI of lungs would provide a sensitive measure of regional ventilation defects in pediatric CF patients. Specifically, we sought to verify that patients with mild CF lung disease exhibited more ventilation defects compared to age-matched controls. Further, by comparing age-matched CF and control groups, we also sought to demonstrate that ^{129}Xe MRI is more sensitive than the clinical gold standard (FEV_1) to detect and quantify mild CF lung disease.

2. Methods

2.1. Approval and subject cohorts

Study approval was obtained from the Cincinnati Children's Hospital Medical Center (CCHMC) Institutional Review Board and via FDA investigational new drug approval (IND 123,577). Informed parental consent and subject assent when appropriate were obtained from 11 healthy control volunteers and 11 cystic fibrosis patients. Inclusion criteria included age between 6 and 17 years old and ability to complete a 16 s breath-hold. Exclusion criteria for all subjects included history of heart defects; symptoms of active respiratory infection, chest tightness, or sinus infection one week prior to MRI; baseline pulse oximetry (SpO_2) ≤ 95% at the time of MRI; and standard MRI exclusions (e.g., claustrophobia, metal implants).

2.2. Spirometry and inhalation dosage

All spirometry was performed according to ATS guidelines [27]. Same-day spirometry was performed by subjects for whom recent (within 6 months) clinical pulmonary function tests were unavailable. For these subjects (all healthy volunteers, and CF subjects #2 and #3), spirometry was performed immediately prior to MRI using a handheld, portable spirometer (Koko, nSpire, Longmont, CO). Inhalation dose with HP ^{129}Xe was 1/6th of a subject's predicted total lung capacity (TLC) calculated using subject height from the ATS plethysmography-based guidelines for children [28]. For boys, TLC in liters is estimated by $TLC = 9.96 \times h^{2.5698} \times 10^{-6}$ and for girls, $TLC = 9.17 \times h^{2.5755} \times 10^{-6}$, where h is the subject height in centimeters [29], with a maximum dose of 1 L. One exception was control #1 who received a dose of 1/12th TLC as per IRB requirement.

2.3. Xenon dose administration

Xenon gas was administered by a trained member of the study staff in the presence of a medical professional (RN or MD). Subjects were coached to fully inhale to TLC and exhale to functional residual capacity (FRC) twice before inhaling the HP ^{129}Xe gas mixture from FRC via a mouthpiece and bag, followed by a breath-hold (up to 16 s) during ^{129}Xe ventilation imaging. Subject heart-rate and SpO_2 were monitored throughout the study via a MR-compatible pulse oximeter (model 865,353 MRI Patient Monitor, InVivo Corporation, Orlando, FL).

2.4. Imaging methods

Subjects were imaged on a Philips Achieva 3 T MRI scanner (Philips Healthcare, Best, Netherlands). Xenon was hyperpolarized either by a commercial polarizer (Polarean, Durham, NC) to 10–14% polarization (100% Xe gas), or a homebuilt polarizer to 24–32% polarization (50% Xe/ 50% N_2 mixture). Note that while the xenon concentration is different between polarizers, the relative signal is constant — an important control for analysis. The gas was transported in a Tedlar bag to the magnet and was administered to each subject for a 10–16 s

breath-hold gradient echo scan (flip angle = 10°–12°, repetition time = 8 ms, echo time = 4 ms, voxel size ≈ 3 × 3 × 15 mm^3, 9–14 slices). Following the scan, the subject was coached to exhale and take several deep breaths to return blood oxygenation to nominal levels. SpO_2 was monitored for at least 2 min following the scan.

Two home-built, saddle-shaped, single-channel transmit/receive MRI coils tuned to 35.3 MHz (^{129}Xe frequency at 3 T) were constructed for use in these experiments [30] and demonstrated relatively flat spatial sensitivity profiles. However, in order to further improve analysis accuracy, signal intensity was calculated in each dimension of the 3D image set (anterior–posterior, left–right, and apex-base) in order to correct for any gradual spatial variation in signal intensity deemed to be the result of coil sensitivity inhomogeneity (not the result of physiological ventilation inhomogeneity).

2.5. Image analysis

Images were analyzed for ventilation defects using custom MatLab (Mathworks) and R software by identifying voxels whose signal intensity was less than 60% of the whole-lung mean signal. The percentage of the lung volume with HP ^{129}Xe signal below this threshold is the ventilation defect percentage (VDP). The threshold of 60% has been used in similar ^{3}He studies in asthma [31] to provide maximum contrast between healthy and diseased lungs and was similarly verified for ^{129}Xe in CF by quantifying whole-lung defect percentage as a function of defect threshold in order to identify the greatest group difference (see Fig. 1). This simple approach reduces potential reader bias and inter-observer variability, since defects were identified by the software. Control patient #5 was imaged twice in succession, once with gas from the homebuilt polarizer and then with gas from the commercial polarizer, in order to verify reproducibility between the two gas mixtures with similar SNR (calculated as mean HP gas signal within lung volume divided by standard deviation of signal outside lung volume).

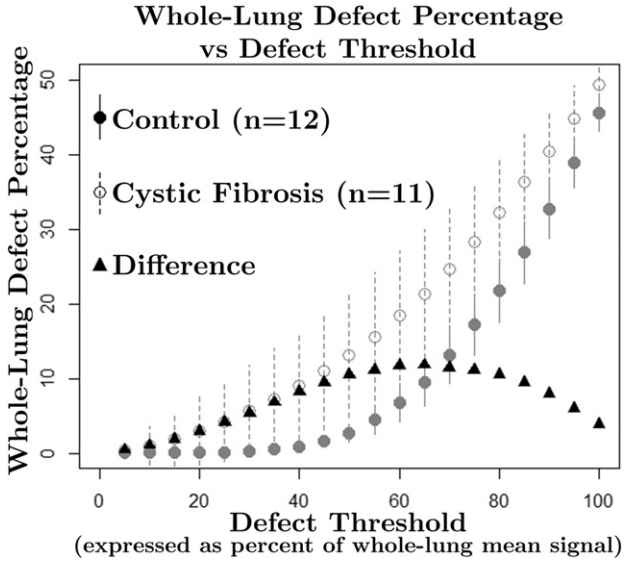

Fig. 1. Plot of whole-lung VDP in control (●) and CF (○) cohorts vs defect threshold. VDP was plotted as a function of defect threshold (expressed as percentage of whole-lung signal mean). The difference between CF and control defect percentages (▲) illustrates the greatest difference near a 60% defect threshold. Lines extending from data points are standard-deviation error bars. Control patient #5 was imaged twice, and both image sets were included here (hence n = 12 for controls).

2.6. Statistical methods

Whole-lung VDP was calculated for each patient for comparison with the measured FEV_1 (percent predicted). Data were analyzed by calculations of means and standard deviations for continuous data, and correlations between two variables were assessed using Pearson correlation coefficients. Student's t-test was used for all reported p-value calculations between groups. A Mann–Whitney–Wilcoxon [Wilcoxon] test was used to evaluate p-values between continuous and categorical values (e.g. FEV_1 and sex). Fisher's test was used to evaluate trends between categorical variables (e.g. controls and sex). p-Values < 0.05 were considered statistically significant.

3. Results

Table 1 summarizes the demographic information of the control and CF populations. The two groups were well matched for age ($p = 0.36$) and sex ($p = 0.39$, by Fisher's exact test), and there were no statistically significant differences observed in the reported parameters. The control group had a higher percentage of male participants compared with the CF subjects. Genotypes of the CF patients were predominately non-functional, and two (subjects CF#4 and CF#7) were pancreatic sufficient (based on fecal elastase testing). Of the 11 CF subjects, 9 grew CF pathogens in respiratory cultures in the year prior to imaging (detailed in Table 1).

HP imaging was well tolerated by all subjects, and no subjects demonstrated a nadir longer than 20 s. Transient desaturations in measured blood oxygenation were noted in most subjects (9 of 11 controls and 9 of 11 CF patients), resolved within 60 s of inhalation, and were not different between CF and controls. Fig. 1 summarizes the relationship between defect threshold and measured VDP. The greatest difference was observed near a 60% defect threshold, which was subsequently used for all image analysis.

All ventilation images demonstrated high image quality for quantitative analysis. Signal-to-noise ratio (SNR) for all subject images averaged 15.9 ± 5.8 (16.8 ± 7.0 for controls, 15.1 ± 4.5 for CF patients, $p = 0.51$) with a minimum SNR of 6.6 for control subject #3. Fig. 2 shows examples of HP ^{129}Xe images in a healthy control and two CF patients with normal and mild obstructive disease (based on FEV_1 percent predicted) for comparison.

Control patient #5 was imaged twice in succession (Fig. 3). The first dose of 50% ^{129}Xe and 50% N_2 at ~32% polarization yielded SNR = 22.9 and VDP = 7.7%, and the second dose of 100% ^{129}Xe at 12% polarization yielded SNR = 18.5 and a VDP = 9.4%. These two VDPs were averaged to yield the reported VDP

Table 1
Demographic description of enrolled subjects. FEV_1 (reported as percent of predicted value) and VDP results (reported as percent of lung volume). Sa = *Staphylococcus aureus*, A = *Achromobacter*, Ca = *Candida albicans*, Sp = *Scedosporium prolificans*, Sm = *Stenotrophomonas maltophilia*, Hi = *Haemophilus influenza*, Pa = *Pseudomonas aeruginosa*.

	Subject	Age [yr]	Sex	Height [cm]	Weight [kg]	CF genotype	Scan/PFT interval [days]	CF pathogen	FEV_1 [%]	VDP [%]
Healthy Controls	1	11	F	149	35.1	-	0	–	100	6.6
	2	7	F	128	33.0	-	0	–	115	4.0
	3	14	M	150	40.6	-	0	–	108	5.8
	4	14	M	177	64.8	-	0	–	106	12.0
	5	12	M	141	34.8	-	0	–	103	7.7
	6	13	M	171	57.2	-	0	–	109	7.8
	7	13	M	160	45.8	-	0	–	89	7.9
	8	12	M	160	23.6	-	0	–	92	4.4
	9	8	M	136	35.2	-	0	–	91	7.2
	10	6	F	116	20.8	-	0	–	95	1.8
	11	16	F	169	49.6	-	0	–	95	4.7
	Mean ± SD	11.5 ± 3.2	64% M	151 ± 19	43.0 ± 19.1		0		100.3 ± 8.5	6.4 ± 2.7
Cystic Fibrosis	1	14	M	167	54.4	F508del, F508del	10	Sa,A,Ca	97	19.3
	2	12	F	162	43.6	F508del, F508del	0	A,Sp	77	31.1
	3	13	F	161	48.9	F508del, G551D	0	–	96	9.6
	4	14	F	156	51.2	F508del, L206 W	28	Sa,Hi	106	5.2
	5	16	M	179	65.5	F508del, F508del	10	Sm	120	14.5
	6	8	M	126	27.8	F508del, F508del	30	Hi	118	18.5
	7	11	M	142	34.5	F508del, R1066H	72	–	102	27.5
	8	13	F	157	46.5	F508del, G178R	1	Hi	114	14.8
	9	15	F	159	43.7	F508del, F508del	8	Sa,Pa	72	32.2
	10	11	F	152	40.1	F508del, F508del	8	Sa	89	13.9
	11	11	F	147	34.3	F508del, F508del	8	Pa	86	15.4
	Mean ± SD	12.5 ± 2.3	36% M	155 ± 14	44.5 ± 10.6		15.9 ± 21.1		97.9 ± 16.0	18.3 ± 8.6
	P values	0.37	0.23	0.52	0.78				0.672	0.0009

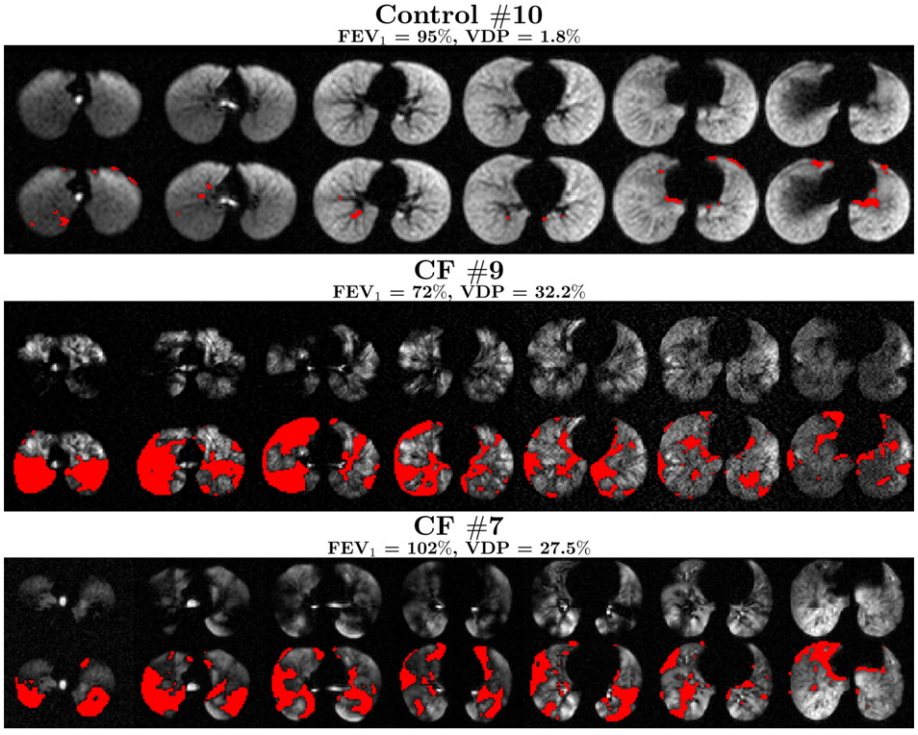

Fig. 2. Axial HP ^{129}Xe MRI slices of Healthy Control #10, CF patient #9 (highest VDP), and CF patient #7 (high FEV_1 and VDP) both with and without defect voxels identified.

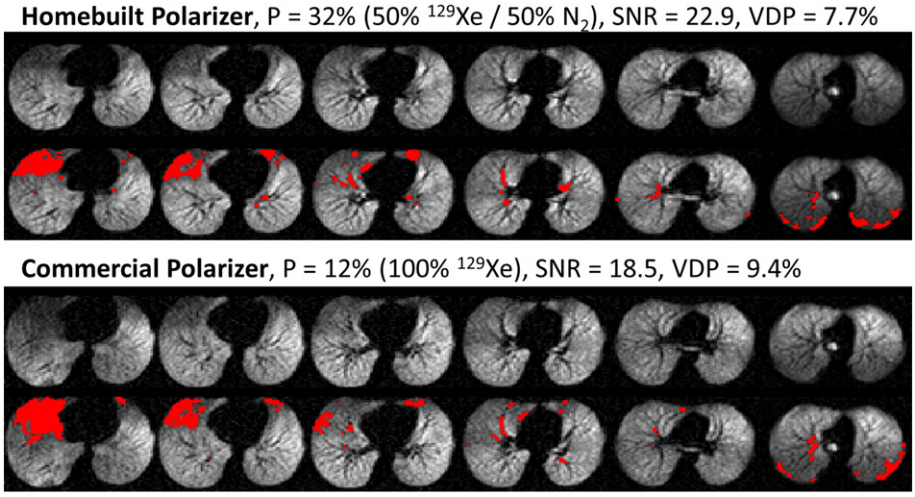

Fig. 3. Hyperpolarized ^{129}Xe images in healthy volunteer #5, with and without defect voxels colored, using ^{129}Xe hyperpolarized in a homebuilt polarizer (top) and commercial polarizer (bottom). Mean VDP for this patient was 8.6% (higher than our mean for controls, detailed in Table 1).

for control #5 (8.6%). Xenon polarizations of the homebuilt polarizer (50/50 mixture) averaged 27.4% ± 2.7%, and the commercial polarizer (100% xenon) averaged 12.2% ± 2.6% (errors are standard deviations). The results indicate that the two polarizing techniques provided gas mixtures with similar SNR and thus similar VDP. In this report, 6 controls and 2 CF subjects were imaged with the first technique (50% ^{129}Xe and 50% N_2), and the remainder with the second technique (100% ^{129}Xe). Both techniques yielded approximately the same net MRI signal.

The mean FEV_1 for the control group was 100.3% ± 8.5% (mean ± sd) and for CF patients was 97.9% ± 16.0% ($p = 0.672$). Whole-lung ^{129}Xe ventilation defect percentage was 6.4% ± 2.7% for controls and 18.3% ± 8.6% for CF ($p = 0.0009$). These are compared graphically in Fig. 4. The Pearson correlation between VDP and FEV_1 across all CF subjects and controls was $r = -0.37$ ($p = 0.087$). Neither FEV_1 nor VDP significantly correlated with age (FEV_1 $r = -0.06$, VDP $r = 0.20$). No significant difference between males and female was exhibited by FEV_1 ($p = 0.13$) or VDP ($p = 0.88$). The correlation between FEV_1 and VDP for the CF subjects was −0.54 ($p = 0.089$). The comparative relationships between FEV_1 and VDP for each subject are also summarized in Table 1.

When the subgroup of CF patients with 'normal' FEV_1 was compared to healthy controls (CF patients with $FEV_1 > 85\%$, $n = 9$, CF#2 and CF#9 excluded), mean FEV_1 of these CF patients was 103.1% ± 12.3% and VDP was 15.4% ± 6.3%; the CF vs control group differences measured by VDP remained statistically significant ($p = 0.002$), while group separation by FEV_1 remained insignificant ($p = 0.57$). Within the CF subjects, 10 of 11 demonstrated VDP values greater than the control average VDP. Only one CF patient showed virtually no defects (CF #4, pancreatic sufficient with a partially functional L206 W conduction mutation in CFTR, FEV_1 = 106% percent predicted).

4. Discussion

Sensitive and functional biomarkers of regional lung disease are critical gaps in CF care and the development of new therapies, particularly in patients with mild disease manifestations. As new therapies improve outcomes, this need becomes

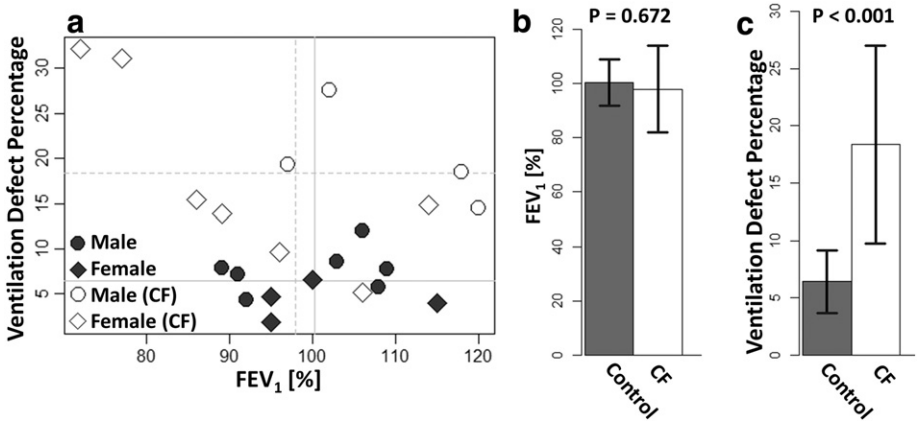

Fig. 4. a: Plot of VDP vs FEV_1 for all subjects (healthy, filled symbols; CF, open symbols) demonstrating the wide range of ventilation defect percentages among the near-normal FEV_1 values. Solid lines are control means, dashed lines are CF means. b: Bar plot showing mean for FEV_1 for control and CF populations. c: Bar plot showing mean VDP for control and CF populations. Error bars are standard deviations. Individual numeric data are provided in Table 1.

more evident, as the capacity to detect the impact of new interventions becomes increasingly difficult with available tools. In the current study, we describe the performance of ^{129}Xe HP MR imaging in pediatric controls and mild CF patients to detect and quantify regional ventilation abnormalities. We hypothesized that this imaging modality could be applied to this population, and that standardized quantification techniques would demonstrate differences between CF patients and healthy controls that were not detectable by standard pulmonary function tests. ^{129}Xe HP MR imaging demonstrated the capacity to detect regional ventilation defects in the vast majority of CF patients despite only minimal lung disease as quantified by FEV_1 percent predicted, which is the current gold standard to monitor CF lung disease status and progression. While the methods described here (simple defect quantification) cannot differentiate CF from other obstructive pulmonary diseases (similar to pulmonary function testing), we believe the technique has high potential for understanding longitudinal changes and response to therapy in individual patients. The ^{129}Xe breath-hold protocol was well tolerated by all subjects; as anticipated from Xe safety studies in adults, mild, transient oxygen desaturations were observed in most subjects and spontaneously resolved with normal breathing of room air. These results demonstrate the power of HP ^{129}Xe MRI to regionally quantify functional ventilation defects in CF, and support further evaluation as a lung disease biomarker and monitoring tool.

Our results indicate that HP ^{129}Xe was considerably more sensitive than FEV_1 in detecting CF lung disease and segregating CF patients from healthy controls. This capacity was sustained when our analysis was limited to CF patients without clear lung disease, and those with mild lung disease (FEV_1 < 85%) were excluded. This is perhaps not surprising as FEV_1 is an effort-dependent measure of global lung function, whereas HP gas MRI reveals regional ventilation during a near-tidal breath hold. These differences have been described in past studies with ^{3}He in older patients [32]. Variability in FEV_1 for healthy control pediatric subjects may be expected to be increased relative to CF patients, as most control subjects have likely never performed pulmonary function tests, whereas CF patients routinely perform spirometry after 6 years of age. The impact of this training effect to provide meaningful spirometry data also becomes problematic in younger CF patients. Unlike FEV_1 however, the sensitivity and regional information obtained by HP gas imaging can be acquired in a single breath hold, and allows unique spatial precision to detect functional deficits that may relate to particular areas of structural abnormalities. The sensitivity of HP ^{129}Xe to detect ventilation abnormalities in this study compared to FEV_1 is particularly encouraging since the mean FEV_1 of the CF subjects did not differ from the controls. Detecting early changes in CF lung disease is critical, since emerging therapies are geared towards preventing or delaying permanent and/or irreversible lung pathologies such as bronchiectasis, and our results support HP ^{129}Xe VDP as a sensitive, functional biomarker to evaluate the efficacy of new therapies in individual CF patients. For example, the lack of ventilation abnormalities in CF #4 is consistent with this patient's pancreatic sufficiency and partially functional L206 W conduction mutation in CFTR. In future studies, ^{129}Xe VDP will be compared to LCI measurements; however, it is important to consider that LCI is a global measurement of lung function and lacks the spatial information from ^{129}Xe MRI.

While CT currently demonstrates the highest achievable structural resolution of all clinical imaging techniques, its ionizing radiation limits its use in longitudinal studies. This is particularly important in the monitoring of pediatric patients [33]. Hyperpolarized ^{129}Xe MRI provides a robust method of investigating regional lung ventilatory function, and recent advancements in proton MRI (e.g., UTE techniques) have improved the visualization of the lung parenchymal structure; in concert, these techniques may provide complementary information to elucidate regional structure–function relationships of lung disease [34]. The moderate negative correlation demonstrated between FEV_1 and VDP ($r = -0.37$) indicates that the two modalities capture related, but not necessarily the same, information. Importantly, our results demonstrate that subjects with normal FEV_1 can have regions of clearly defective ventilation. It is also notable that ^{129}Xe gas has the potential to detect and quantify other functional measures in the lung, including diffusion within parenchymal airspaces for airspace size measurement [35], and gas exchange across the alveolar barrier [36,37]. These techniques may provide complementary information to conventional structural imaging or HP gas ventilation imaging relating to CF pathology. For example, it has been shown that perfusion MRI is sensitive to early CF lung disease [38], and ^{129}Xe MRI gas-exchange methods may provide an alternative to avoid intravenous gadolinium-based contrast agents.

There are also limitations of the work. First, the number of subjects enrolled was relatively small and was primarily limited to pediatric patients with normal or mild lung disease. Subsequent studies will be needed to determine the role of ^{129}Xe MR imaging in more advanced CF lung disease; however, the small cohort size in this study demonstrates the sensitivity of ^{129}Xe VDP to detect early CF lung disease and provides robust group separation. This increased sensitivity may be particularly important in clinical trials for emerging CF therapies targeting rare CF genotypes. Second, the studies were cross-sectional, and did not assess the longitudinal performance of HP ^{129}Xe VDP over time (during either periods of disease stability or instability). Studies of this nature will be critical to determine the future role of ^{129}Xe in disease monitoring or as a biomarker of intervention. In addition, subjects with lower SNR may arguably have artificially elevated VDP since a single threshold was used for defect identification. The subjects with the lowest SNR, however, were controls (control #3, SNR = 6.6, VDP = 5.8%; control #4, SNR = 7.7, VDP = 12.0%). Because there was no significant difference in SNR between the control and CF groups ($p = 0.6$), this limitation does not likely affect its sensitivity to detect regional CF lung disease. Finally, hyperpolarized ^{129}Xe is currently classified by the FDA as an investigational new drug, and thus requires FDA approval for use in clinical trials or disease management.

These results provide strong support to investigate the future role of ^{129}Xe MR imaging in clinical trials, particularly those

focused on evaluating new therapies for CF patients with mild disease. This is a vital consideration, as patients who do not have established structural lung disease are likely to receive the greatest benefit from transformative therapies such as CFTR modulators [39,40]. Here we have demonstrated the efficacy of hyperpolarized ^{129}Xe to detect regional lung defects in pediatric patients with minimal CF lung disease. The sensitivity of ^{129}Xe to quantitatively differentiate healthy subjects from mild CF was readily apparent utilizing our relatively simple defect identification threshold. These findings indicate that HP ^{129}Xe imaging may be a useful tool to detect and monitor disease progression, and to quantify individual responses to individualized treatments. ^{129}Xe MRI may also reveal relationships between various CF structural pathologies (bronchiectasis, mucus plugging, etc.) and regional ventilation. As more specialized clinical trials develop and CF phenotypic differences become more defined, combining clinical measures with regional ventilation may aid in the development of more effective treatments and understanding individual responses to those treatments.

Author contributions

Concept and design: RPT, LLW, DJR, ZIC, JPC, JCW. Analysis and interpretation: RPT, LLW, DJR, ZIC, JPC, JCW. All authors contributed to the intellectual content of the manuscript.

Support

T32 HL007752.

References

[1] Ikpa PT, Bijvelds MJ, de Jonge HR. Cystic fibrosis: toward personalized therapies. Int J Biochem Cell Biol 2014;52:192–200.
[2] World Health Organization. The molecular genetic epidemiology of cystic fibrosis human genetics programme: chronic diseases and health promotion; 2004.
[3] O'Sullivan BP, Freedman SD. Cystic fibrosis. Lancet 2009;373(9678):1891–904.
[4] Rowe SM, Heltshe SL, Gonska T, Donaldson SH, Borowitz D, Gelfond D, et al. Network GIotCFFTD. Clinical mechanism of the cystic fibrosis transmembrane conductance regulator potentiator ivacaftor in G551D-mediated cystic fibrosis. Am J Respir Crit Care Med 2014;190(2):175–84.
[5] de Jong PA, Ottink MD, Robben SG, Lequin MH, Hop WC, Hendriks JJ, et al. Pulmonary disease assessment in cystic fibrosis: comparison of CT scoring systems and value of bronchial and arterial dimension measurements. Radiology 2004;231(2):434–9.
[6] Gai ND, Malayeri A, Agarwal H, Evers R, Bluemke D. Evaluation of optimized breath-hold and free-breathing 3D ultrashort echo time contrast agent-free MRI of the human lung. J Magn Reson Imaging 2015.
[7] Soni R, Dobbin CJ, Milross MA, Young IH, Bye PP. Gas exchange in stable patients with moderate-to-severe lung disease from cystic fibrosis. J Cyst Fibros 2008;7(4):285–91.
[8] Aebischer CC, Kraemer R. The lung clearance index (LCI) as an estimate of ventilation inequalities in patients with cystic fibrosis. Agents Actions Suppl 1993;40:73–83.
[9] Stanojevic S, Jensen R, Sundaralingam D, Salazar JG, Yammine S, Singer F, et al. Alternative outcomes for the multiple breath washout in children with CF. J Cyst Fibros 2015;14(4):490–6.
[10] Roos JE, McAdams HP, Kaushik SS, Driehuys B. Hyperpolarized gas MR imaging: technique and applications. Magn Reson Imaging Clin N Am 2015;23(2):217–29.
[11] Couch MJ, Blasiak B, Tomanek B, Ouriadov AV, Fox MS, Dowhos KM, et al. Hyperpolarized and inert gas MRI: the future. Mol Imaging Biol 2015;17(2):149–62.
[12] Flors L, Altes TA, Mugler III JP, de Lange EE, Miller GW, Mata JF, et al. New insights into lung diseases using hyperpolarized gas MRI. Radiologia 2015;57(4):303–13.
[13] Koumellis P, van Beek EJ, Woodhouse N, Fichele S, Swift AJ, Paley MN, et al. Quantitative analysis of regional airways obstruction using dynamic hyperpolarized 3He MRI-preliminary results in children with cystic fibrosis. J Magn Reson Imaging 2005;22(3):420–6.
[14] van Beek EJ, Hill C, Woodhouse N, Fichele S, Fleming S, Howe B, et al. Assessment of lung disease in children with cystic fibrosis using hyperpolarized 3-helium MRI: comparison with Shwachman score, Chrispin-Norman score and spirometry. Eur Radiol 2007;17(4):1018–24.
[15] McMahon CJ, Dodd JD, Hill C, Woodhouse N, Wild JM, Fichele S, et al. Hyperpolarized 3helium magnetic resonance ventilation imaging of the lung in cystic fibrosis: comparison with high resolution CT and spirometry. Eur Radiol 2006;16(11):2483–90.
[16] Donnelly LF, MacFall JR, McAdams HP, Majure JM, Smith J, Frush DP, et al. Cystic fibrosis: combined hyperpolarized 3He-enhanced and conventional proton MR imaging in the lung — preliminary observations. Radiology 1999;212(3):885–9.
[17] O'Sullivan B, Couch M, Roche JP, Walvick R, Zheng S, Baker D, et al. Assessment of repeatability of hyperpolarized gas MR ventilation functional imaging in cystic fibrosis. Acad Radiol 2014;21(12):1524–9.
[18] Kirby M, Svenningsen S, Ahmed H, Wheatley A, Etemad-Rezai R, Paterson NA, et al. Quantitative evaluation of hyperpolarized helium-3 magnetic resonance imaging of lung function variability in cystic fibrosis. Acad Radiol 2011;18(8):1006–13.
[19] Paulin GA, Svenningsen S, Jobse BN, Mohan S, Kirby M, Lewis JF, et al. Differences in hyperpolarized (3) He ventilation imaging after 4 years in adults with cystic fibrosis. J Magn Reson Imaging 2015;41(6):1701–7.
[20] Mentore K, Froh DK, de Lange EE, Brookeman JR, Paget-Brown AO, Altes TA. Hyperpolarized HHe 3 MRI of the lung in cystic fibrosis: assessment at baseline and after bronchodilator and airway clearance treatment. Acad Radiol 2005;12(11):1423–9.
[21] Woodhouse N, Wild JM, van Beek EJ, Hoggard N, Barker N, Taylor CJ. Assessment of hyperpolarized 3He lung MRI for regional evaluation of interventional therapy: a pilot study in pediatric cystic fibrosis. J Magn Reson Imaging 2009;30(5):981–8.
[22] Bannier E, Cieslar K, Mosbah K, Aubert F, Duboeuf F, Salhi Z, et al. Hyperpolarized 3He MR for sensitive imaging of ventilation function and treatment efficiency in young cystic fibrosis patients with normal lung function. Radiology 2010;255(1):225–32.
[23] Sun Y, O'Sullivan BP, Roche JP, Walvick R, Reno A, Baker D, et al. Using hyperpolarized 3He MRI to evaluate treatment efficacy in cystic fibrosis patients. J Magn Reson Imaging 2011;34(5):1206–11.
[24] Driehuys B, Martinez-Jimenez S, Cleveland ZI, Metz GM, Beaver DM, Nouls JC, et al. Chronic obstructive pulmonary disease: safety and tolerability of hyperpolarized 129Xe MR imaging in healthy volunteers and patients. Radiology 2012;262(1):279–89.
[25] Walkup LL, Thomen RP, Akinyi T, Watters E, Ruppert K, Clancy JP, et al. Feasibility, tolerability, and safety of pediatric hyperpolarized ^{129}Xe magnetic resonance imaging in healthy volunteers and subjects with cystic fibrosis. Pediatr Radiol 2016. http://dx.doi.org/10.1007/s00247-016-3672-1.
[26] Kirby M, Ouriadov A, Svenningsen S, Owrangi A, Wheatley A, Etemad-Rezai R, et al. Hyperpolarized ^{3}He and ^{129}Xe magnetic resonance imaging apparent diffusion coefficients: physiological relevance in older never- and ex-smokers. Physiol Rep 2014;2(7).
[27] Miller MR, Hankinson J, Brusasco V, Burgos F, Casaburi R, Coates A, et al. Standardisation of spirometry. Eur Respir J 2005;26(2):319–38.
[28] Stocks J, Quanjer PH. Reference values for residual volume, functional residual capacity and total lung capacity. ATS Workshop on Lung Volume Measurements. Official Statement of the European Respiratory Society. Eur Respir J 1995;8(3):492–506.

[29] Zapletal A, Paul T, Samanek M. Significance of contemporary methods of lung function testing for the detection of airway obstruction in children and adolescents (author's transl). Z Erkr Atmungsorgane 1977;149(3): 343–71.
[30] Loew W, Thomen R, Pratt R, Cleveland ZI, Dumoulin C, Woods JC, et al. A volume saddle coil for hyperpolarized ^{129}Xe lung imaging. Proc Int Soc Magn Reson Med 2015;23:1507.
[31] Thomen RP, Sheshadri A, Quirk JD, Kozlowski J, Ellison HD, Szczesniak RD, et al. Regional ventilation changes in severe asthma after bronchial thermoplasty with (3)He MR imaging and CT. Radiology 2015;274(1): 250–9.
[32] Quirk JD, Chang YV, Yablonskiy DA. In vivo lung morphometry with hyperpolarized (3) He diffusion MRI: reproducibility and the role of diffusion-sensitizing gradient direction. Magn Reson Med 2015;73(3): 1252–7.
[33] de Jong PA, Nakano Y, Lequin MH, Mayo JR, Woods R, Pare PD, et al. Progressive damage on high resolution computed tomography despite stable lung function in cystic fibrosis. Eur Respir J 2004;23(1):93–7.
[34] Ruppert K, Mata JF, Brookeman JR, Hagspiel KD, Mugler III JP. Exploring lung function with hyperpolarized (129)Xe nuclear magnetic resonance. Magn Reson Med 2004;51(4):676–87.
[35] Kirby M, Svenningsen S, Owrangi A, Wheatley A, Farag A, Ouriadov A, et al. Hyperpolarized ^{3}He and ^{129}Xe MR imaging in healthy volunteers and patients with chronic obstructive pulmonary disease. Radiology 2012; 265(2):600–10.
[36] Mugler III JP, Altes TA, Ruset IC, Dregely IM, Mata JF, Miller GW, et al. Simultaneous magnetic resonance imaging of ventilation distribution and gas uptake in the human lung using hyperpolarized xenon-129. Proc Natl Acad Sci U S A 2010;107(50):21707–12.
[37] Freeman MS, Cleveland ZI, Qi Y, Driehuys B. Enabling hyperpolarized (129) Xe MR spectroscopy and imaging of pulmonary gas transfer to the red blood cells in transgenic mice expressing human hemoglobin. Magn Reson Med 2013;70(5):1192–9.
[38] Fleck R, McPhail G, Szczesniak R, Knowlton J, Radhakrishnan R, Clancy J, et al. Aortopulmonary collateral flow in cystic fibrosis assessed with phase-contrast MRI. Pediatr Radiol 2013;43(10):1279–86.
[39] Wainwright CE. Ivacaftor for patients with cystic fibrosis. Expert Rev Respir Med 2014;8(5):533–8.
[40] Altes TA, Johnson M, Higgins M, Fidler M, Botfield M, Mugler III JP, et al. The effect of ivacaftor treatment on lung ventilation defects, as measured by hyperpolarized helium-3 MRI, on patients with cystic fibrosis and a G551D-CFTR mutation. J Cyst Fibros 2014;13 [Abstracts of the 37th European Cystic Fibrosis Conference].